

IJSGS



ISSN: 2488-9229  
FEDERAL UNIVERSITY  
GUSAU-NIGERIA

## INTERNATIONAL JOURNAL OF SCIENCE FOR GLOBAL SUSTAINABILITY

### Determination of Geothermal Potential of Lower Sokoto Basin, North-Western Nigeria Using High Resolution Aeromagnetic Data

Badamasi Umar<sup>1</sup>, Danladi Bonde<sup>2</sup>, Abdullateef Aliyu<sup>3</sup>, Zayyanu Hussaini Imam<sup>4</sup>, Imrana Alhaji<sup>1</sup>

Umaru Ali Shinkafi Polytechnic, Sokoto<sup>1</sup>

Kebbi State University of Science and Technology Aliero<sup>2</sup>

Federal University of Technology, Minna<sup>3</sup>

Federal University of Agriculture, Zuru<sup>4</sup>

Corresponding Author's Email: [abdullateefaliyu57@gmail.com](mailto:abdullateefaliyu57@gmail.com)

Received on: August, 2022

Revised and Accepted on: September, 2022

Published on: October, 2022

#### ABSTRACT

This research deals with determination of geothermal potential of lower Sokoto Basin, north-western Nigeria using four (4) high resolution aeromagnetic data covering the study area (area bounded by latitude 11.0<sup>0</sup>N to 12.0<sup>0</sup> N and longitude 4.50<sup>0</sup>E to 5.50<sup>0</sup>E). Depth estimates were made from the spectral analysis of the magnetic anomalies. The polynomial fitting was utilized to suppress the short wavelength components (regional magnetic anomaly of the total magnetic field) in the Sokoto Basin. The residual of the total magnetic field map was then subjected to spectral depth analysis by dividing it into twenty eight (28) overlapping spectral blocks. The log of spectral energies of each blocks were plotted against frequency. The centroid depth ( $Z_0$ ) and depth to top of magnetic boundary ( $Z_t$ ) obtained from the plots were used to estimate the Curie point depth isotherm, which was then used to compute geothermal heat flow of the study area. An estimated depth of 4.69 km to 11.9 was observed for centroid depth( $Z_0$ ) while the sedimentary thickness (depth to basement,  $Z_b$ ) ranges from 1.29 km to 2.94 km. The result shows that the Curie point depth  $Z_b$  ranges between 7.88km and 22.11km with the highest value found at the North-Eastern while lower values are located at the western part with lowest at the central part of the west. For the geothermal heat flow, it varies between 65.84mW/m<sup>2</sup> and 184.74 mW/m<sup>2</sup>, The geothermal heat flow obtained from this study indicates that the study area possess a good source of geothermal potential. Thus, harnessing the geothermal potential in this area would be of added values and advantage to power generation in Nigeria.

**Keywords:** lower Sokoto Basin, Curie point depth isotherm, spectral blocks

## 1.0 INTRODUCTION

### 1.1 Background of the study

Energy appears to be one of the most crucial issues for every society, international politics, economic spectrum, and the environment. Its finite existence has major effects on mechanisms of decision-making, and the extensive use of fossil fuels has a dominant effect on all aforementioned issues. This results to direct and indirect effects on human activities, particularly human health and welfare most importantly, with environmental issues. But because of their abundance, low cost, and easy use, fossil fuels are still considered by many as irreplaceable choices even though their use causes damage to the environment, Dincer (2010).

Therefore, clean and cost-competitive renewable energy sources such as geothermal are expected to

be potential alternatives to achieve long-term and sustainable solutions.

Geothermal energy has been used for thousands of years; people utilized hot springs for cleaning since the beginning of civilization in all over the world Fridleifsson (2003). Since more than 90% of the Earth's temperature is higher than 100<sup>0</sup>C, geothermal energy can be considered as one of the most abundant resources as an alternative to fossil fuel-based heating-power production applications. Aside from being one of the cheapest energy source (Farhan, 2013), it is a standout amongst the most clean, save sustainable power source that is expensive but easy to maintain and environmental favourable (negligible emissions of CO<sub>2</sub>, SO<sub>2</sub>, NO<sub>2</sub>, and particulates, and modest land and water use).

Records such as Nwankwo and Shehu (2015), Ofor and Udensi (2014) had shown that there is minimal

record of geophysical studies on regional geothermal structure in the lower Sokoto basin. And literatures such as Mijgan (2005), Eleta and Udensi (2012), Megwara *et al.*, (2013) and Ofor and Udensi (2014) have shown that spectral analytical method of magnetic data can be regarded as a proxy for an estimate of Curie-point depth, and geothermal heat flow of a region. In this research we aim to assess the geothermal potential of the lower sokoto basin, borth-Western Nigeria for possible geothermal utilisation and exploration, using spectral depth analysis of aeromagnetic method. The greatest potential for this magnetic method is its ability to detect the depth with certain critical temperature (Curie point) at which magnetic minerals loses their ferromagnetism (approximately 580 °C for magnetite at atmospheric pressure).

**1.2 Geology of the Study Area**

The study area is part of the Sokoto Basin, in northwestern Nigeria (Figure1). Sokoto Basin is predominantly consists of a gently undulating plain with an average elevation varying from 250 to 400m above mean sea-level (Obaje, 2009) and (Odebode, 2010). This plain is occasionally interrupted by low mesas. A low escarpment, known as the “Dange Scarp” is the most prominent feature in the basin and it is closely related to the

geology (Odebode, 2010). The Sokoto (Sedimentary) Basin forms the south-eastern segment of a large synclinal basin that is known as the Iullemeden basin. The Iullemeden basin lies entirely within the Pan African province of West Africa; which encompasses parts of Algeria, Mali, and Republic of Benin and Niger (Odebode, 2010). Additionally, found in the basin (figure 1) are sequences of sands, clay, some limestone and ironstone, and semi consolidated gravels. It consists of about 60% of the sedimentary and 40% of basement (Zboril, 1984). The sedimentary sequences are subdivided into late Jurassic to early Cretaceous Illo and Gundumi Formation, the Maestrichtian Rima Group, the late Paleocene Sokoto Group and the Eocene-Miocene Gwandu Formation (Kogbe, 1979 and 1981).

Kogbe (1979) described Sokoto basin as a series of crystalline massif rocks outcropping to the east and south of the basin consisting of granite gneisses, schist, phyllites, quartzites and some amphibolite, diorite, gabbro and marble of pre-Cambrian age. The lowlands and plains of the basement areas are sometimes covered on the surface by Quaternary sediments of Aeolian and fluvial origin especially along the flood plains of the major rivers and streams.

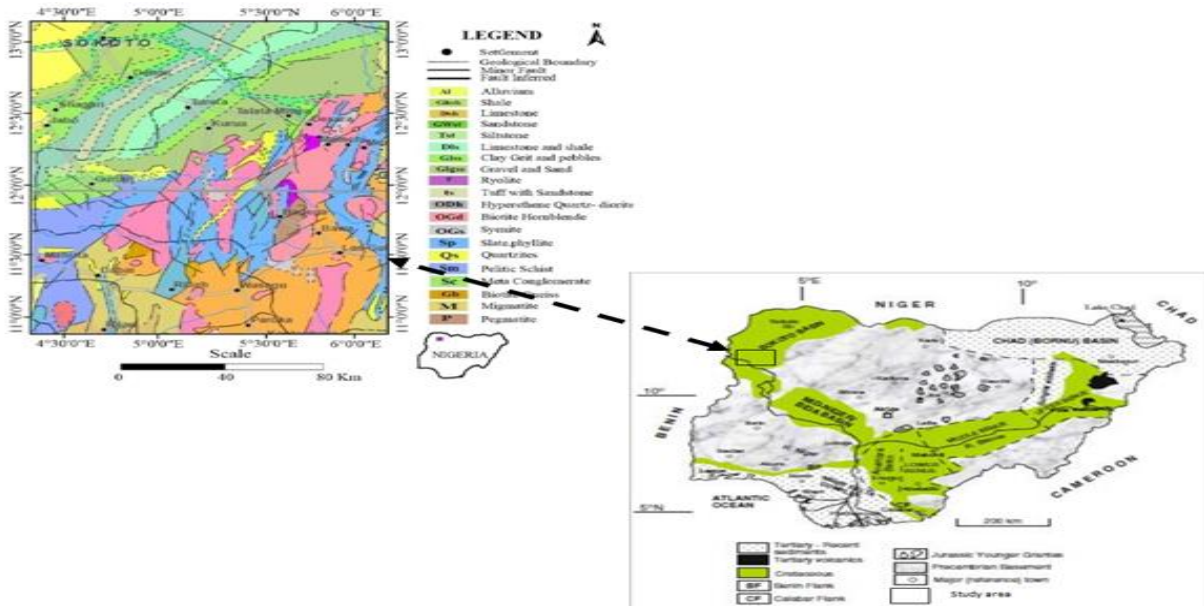


Figure 1: Geological Map of Nigeria showing the study area area in black outline (Source: Obaje, 2009)

## 2.0 MATERIALS AND METHODS

Four digitized aeromagnetic data sheets 73 (Fokku), 74 (Donko), 96 (shanga) and 97 (Wudil) were acquired, assembled for the work. These data were procured from the Nigeria Geological Survey Agency, NGSA as part of the Data NGSA collected from the airborne magnetic survey carried out in the year 2009 by Fugro.

The data were acquired along a series of NW-SE flight with a spacing of 2 km and an average flight elevation of about 150 m while tie lines occur at about 20 km interval. The area covered is about 12,100 km<sup>2</sup>. Using Oasis software, the first step in this study was to assemble the four maps covering the area. The next step was to contour the data to produce the total field aeromagnetic intensity map. Furthermore, the contoured total-field intensity map contains both the regional and residual anomaly. The regional gradient was removed from the map by fitting a linear surface to the digitized aeromagnetic data using a polynomial fitting techniques. The residual anomaly map was later subjected to spectral analysis.

### 2.1 Spectral Depth Analysis

It is a depth estimating method used in geophysics. It is used in investigating the thermal frame work via aeromagnetic studies. Spectral depth analysis based on statistical models has been employed in numerous geophysical works, as in the determination of average depth to the top of magnetic basement and in the computation of crustal thickness. The method discovered by Bhattacharyya (1966) and later developed by (Spector and Grant, 1970) has been utilized widely in the analysis of magnetic anomalies. It depends on the expression of Power spectrum for the total magnetic field anomaly. In this technique various (more than one) anomaly can be utilised to compute the depth to buried magnetic materials.

The technique permits an estimate of depth of magnetized blocks of varying depth, width, thickness and magnetisation. Most approaches used include Fourier transformation of the aeromagnetic data to estimate the energy (or amplitude) spectrum. The energy spectrum is then plotted on the Logarithm scale against frequency. The plot shows the straight line graph which diminish in

slope with rising frequency. The slopes of the segments yield estimates of depths to magnetic sources Aliyuet *al.*, (2018).

Hence, a plot of the energy spectrum of a single ensemble of prism against angular frequency would yield a straight line graph whose slope is directly proportional to the average sourcedepth,  $h$  of that ensemble. That is, the logarithm plot of the radial would yield a straight line whose slope,

$$m = -2h$$

$$h = -\frac{m}{2} \quad (1)$$

Equation (1) can be specifically applied if the frequency unit is in radian per unit distance (kilometer as it is in this research), if it is unit is in cycle per unit distance as it is in this work, the expression becomes

$$h = -\frac{m}{4\pi} \quad (2)$$

### 2.2 Curie Point Depth Estimation

The bottom of a magnetic source indicates the thermal boundary at which magnetic mineral in the crust moves from ferromagnetic status to paramagnetic as a result of the increase in temperature as depth increases down the crust (Nagata, 1961; Ross et al., 2006). This thermal boundary is referred to as Curie point depth and it is the nethermost part of the crust to have material which develops discernible mark in a magnetic anomaly map. (Bhattacharyya and Leu, 1975). This Curie point has a temperature of 550 °C ± 30 °C. For temperature above Curie-point, magnetic materials lose their magnetic ordering and both induced and remnant magnetization disappear, thus for temperatures above 580°C, those materials will begin to encounter ductile deformation.

The Curie point depth is evaluated in two stages as proposed by Bhattacharyya and Leu (1975); the first stage is the estimation of depth to centroid  $h_0$ , of magnetic source from the slope of the longest wavelength part of the spectrum, using Equation (3) (Okubo *etal.*, 1985 and 1989; Eletta and Udensi, 2012; Aliyuet *al.*, 2018).

$$\ln \left[ \frac{\sqrt{p(s)}}{|s|} \right] = \ln A - 2\pi |s| h_0 \quad (3)$$

where

$P(s)$  = radially averaged power spectrum of the anomaly,

$s$  = the wave number,

and  $A$  = constant.

The second stage is the estimation of the depth to the top boundary  $h_1$  from the slope of the second longest wavelength part of the spectrum (Okubo *et al.*, 1985 and 1989; Eletta and Udensi, 2012; Aliyu *et al.*, 2018; Salako *et al.*, 2020)

$$\ln\sqrt{[p(s)]} = \ln B - 2\pi|s|h_1 \quad (4)$$

where  $B$ , is the sum of constant independent of  $|s|$ .

The basal depth  $h_b$  which is assumed to be the Curie point depth of the magnetic source was calculated from the equation below. (Okubo *et al.*, 1985 and 1989; Eletta and Udensi, (2012)

$$h_b = 2h_0 - h_1 \quad (5)$$

The application of Equation (5) was being carried after making two different spectral plots using Equation (3) and (4) for the estimation of the depths to the top or basin thickness ( $h_1$ ) and centroid ( $h_0$ ) of magnetic sources for each block.

In this research the curie-point depth is the obtained basal depth,  $h_b$  of the magnetic source,  $h_0$  is the centroid depth and  $h_1$  is the thickness of basin (basement depth).

### 2.3 Geothermal Gradient and Heat Flow

The fundamental relation for conductive heat movement is Fourier's law (Tanaka *et al.*, 1999). In one-dimensional case under the notions that the direction of the temperature change is vertical and the temperature gradient ( $\frac{dT}{dz}$ ) is constant, Fourier's law is expressed as given in equation (6) (Tanaka *et al.*, 1999; Kasidi and Nur, 2012; Oforand Udensi, 2014)

$$q = -k \frac{dT}{dz} \quad (6)$$

where

$q$  = the heat flux (heat transfer per unit time)

$k$  = coefficient of thermal conductivity.

From Tanaka *et al.*, (1999), the Curie temperature ( $\theta$ ) can then be estimated from the expression

$$\theta = \left(\frac{dT}{dz}\right)h_b$$

$$\frac{dT}{dz} = \left(\frac{\theta}{h_b}\right) \quad (7)$$

Making  $\frac{dT}{dz}$  the subject of the formula in equation (7) and (8) and comparing the result will give

$$h_b = \theta \frac{k}{q} \quad (8)$$

Equation (8) shows that Curie point depth is inversely proportional to heat flow and it signifies that areas of high heat flow experience shallower Curie point depth, on the other hands, those with relatively low heat flow have deeper Curie point depth (Tanaka *et al.*, 1999; Ross *et al.*, 2006). An average surface heat flow value was estimated using Equations (7) and (8) and was predicated on possible Curie temperature of 580°C and thermal conductivity of 2.5  $\text{Wm}^{-1}\text{C}^{-1}$  as suggested by Stacey (1977) as the average for thermal conductivity igneous rocks.

## 3. RESULTS AND DISCUSSION

### 3.1 Total Magnetic Intensity (TMI)

The total magnetic intensity map (TMI) of the study area (Figure 4.1) shows variation of highs and lows in magnetic signature, ranging from -55.6nT to 91.2nT (33000nT have been removed by the NGSAs for proper handling so, to get the actual value, a background value of 33000nT must be added to each value to get the actual value). The pink colouration depicts high magnetic signature while blue depicts low magnetic signature, greenish depicts alluvium deposition and yellow indicates intermediary. The high magnetic signature region denoted with **H** is well pronounced at the south-western part of the of the study area, trending West-East, it could also be found in part of the North-western and central part. Although the low magnetic signatures denoted with **L** is well pronounced in the eastern (especially the South eastern) part of the study area trending NE-SW, it scattered all round the study area.

#### 3.1.1 Residual Map

The residual magnetic intensity map (Figure 4.2) of the study area shows that the area is made up of magnetic intensity values ranges from -72.8 nT to 42.0 nT. The negative values imply areas that are magnetically subdued or quiet while the positive values are magnetically responsive. The magnetically subdued areas are the magnetic lows of the study area and this is typical of a sedimentary terrain while the magnetic responsive areas are the magnetic highs regions which are assumed to be due to the likely presence of outcrops of crystalline

igneous or metamorphic rocks, deep seated volcanic rocks or even crustal boundaries. The high magnetic anomaly which can probably be attributed to igneous intrusion and shallower sediment is well pronounced in the South- Eastern part trending approximately South-East. The high magnetic signature can also be found in the central part trending North-West and the extreme of North-West while the low magnetic anomalies associated with the sedimentary region was well pronounced in Eastern, while other scattered at the central part of the study area.

About one third of the map can be seen to be greenish (featureless) which may correspond to alluvium deposition in the western part of the study area.

The varying amplitude of these magnetic anomalies is an indication of different sedimentary thickness in the study area. These variations in the anomaly amplitude may also indicate possibly the occurrences of basement complex rocks containing varying amounts of magnetic minerals.

At some places on the southern part of the residual map (Figure 4.2) there are anomalies that are not present on the total magnetic map (Fig. 4.1). These anomalies are due to magnetic source of shallow origin.

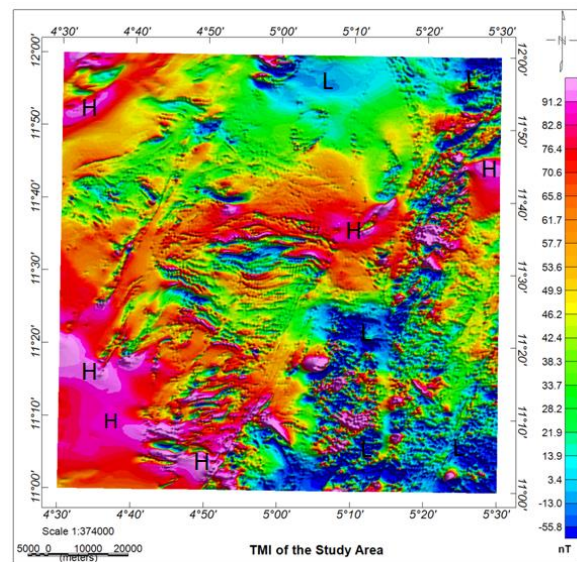


**Figure 4.1: TMI anomaly contour map of the study area (add a background value of 33000nT to each value to get the actual value)**

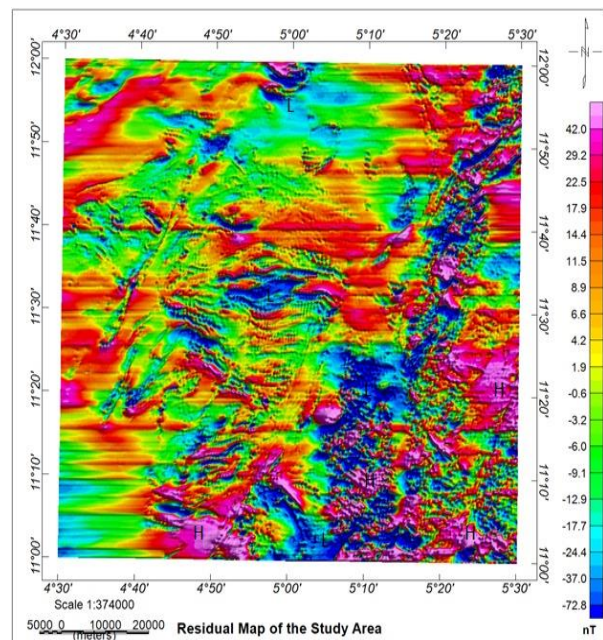


**Figure 4.2: Residual map of the study area**

### 3.2.1 Spectral Analysis

The residual map (Figure 4.2) of the study area was divided into twenty four (Blocks 1 - 24) overlapping magnetic sections. In doing this division we ensured that essential parts of anomaly were not cut by the blocks.

The divisions of residual map into spectral sections or blocks were done with Oasis Montaj. Graph of the logarithm of spectral energies against frequencies obtained for blocks 1 and 2 are shown in (Figure 4.3). The estimated value for centroid depth and depth to top of magnetic basement shown in Table 4.1

From the table 4.1 in line with equation 3.3 an estimated depth of 4.69 km to 11.9 km could be observed for centroid depth while the (depth to basement) ranges from 1.29 km to 2.94 km

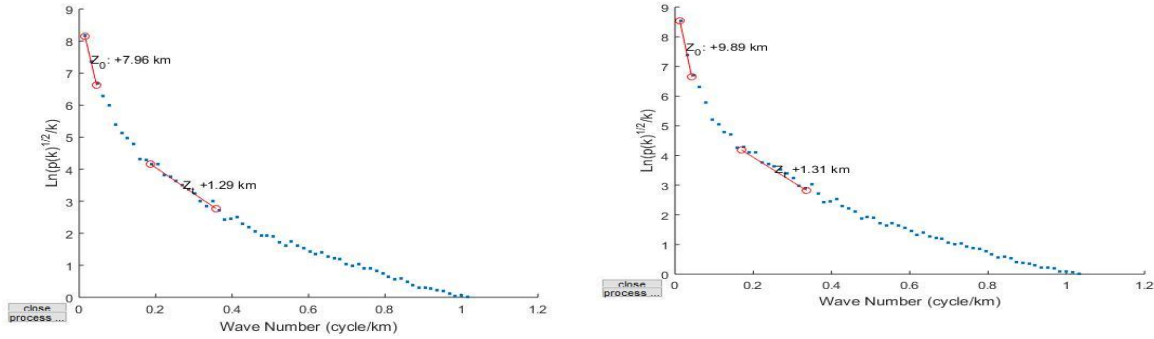


Figure. 4.3:plot the logarithm of spectral energies against frequencies obtained for block 1 and 2.

The contour map for the centroid depth and depth to top of basement are shown in figure 4.4 and 4.5 respectively.

Table 4.1: Location and Depth Estimation of Centroid Depth ( $H_0$ ), Depth to Basement ( $H_t$ ), CPD ( $H_b$ ), Geothermal Gradient and Heat Flow

Block	Long (Deg.)	Lat (Deg.)	$h_0$ (Km)	$h_t$ (Km)	$h_b$ (Km)	$G_g$ ( $^{\circ}C/km$ )	$H_F$ ( $mWm^{-2}$ )
1	4.75	11.75	4.69	1.5	7.88	73.60	184.74
2	4.83	11.75	7.96	1.29	14.63	39.64	99.50
3	4.91	11.75	9.89	1.31	18.47	31.40	78.81
4	5.00	11.75	9.82	1.33	18.31	31.67	79.50
5	5.08	11.75	11.9	1.69	22.11	26.23	65.84
6	5.16	11.75	10.3	2.13	18.47	31.40	78.81
7	5.25	11.75	10.9	2.06	19.74	29.38	73.74
8	4.75	11.58	7.20	1.8	12.6	46.03	115.53
9	4.83	11.58	6.38	2.01	10.75	53.95	135.42
10	4.91	11.58	8.81	2.2	15.42	37.61	94.40
11	5.00	11.58	11.2	1.97	20.43	28.38	71.25
12	5.08	11.58	7.55	2.11	12.99	44.64	112.07
13	5.16	11.58	7.55	2.1	13	44.61	111.98
14	5.25	11.58	7.68	2.02	13.34	43.47	109.13
15	4.75	11.41	7.55	1.75	13.35	43.44	109.04
16	4.83	11.41	7.32	1.92	12.72	45.59	114.44
17	4.91	11.41	7.85	1.88	13.82	41.96	105.34
18	5.00	11.41	10.6	1.86	19.34	29.98	75.27
19	5.08	11.41	9.06	2.12	16	36.25	90.98
20	5.16	11.41	9.82	2.21	17.43	33.27	83.52
21	5.25	11.41	11.2	2.05	20.35	28.50	71.53
22	4.75	11.25	8.48	2.94	14.02	41.36	103.83

23	4.83	11.25	9.69	2.5	16.88	34.36	86.24
24	4.91	11.25	7.83	2.28	13.38	43.34	108.80
25	5.00	11.25	7.55	2.37	12.73	45.561	114.35
26	5.08	11.25	8.06	2.52	13.6	42.64	107.04
27	5.16	11.25	10.6	2.25	18.95	30.60	76.82
28	5.25	11.25	9.23	2.08	16.38	35.40	88.876

### 3.2.2 Curie Point Depth

The results of the spectral analysis of aeromagnetic anomalies over the area shows that the Curie point depth estimates (using equation 5) range between 7.88km and 22.11km (Table 4.1).

The Curie point depth ( $Z_b$ ) map of the study area (figure 4.6) shows that the depth ranged from 21.5km to 14km in the North-Eastern part dipping towards the central, in the western part of the study area the  $Z_b$  ranges between 8 km and 19km increasing towards the central part. By contrast, higher values are located at the Eastern part with highest at the North-Eastern while lower values are located at the western part with lowest at the central part of the west. This Curie point depth result is in agreement with Ofor and Udensi (2014) which suggested that the Sokoto basin is underlain by a Curie-point isotherm of between 11.36 to 22.30km

### 3.2.3 Geothermal Gradient

Using a Curie temperature of 580°C and the estimated Curie point depths geothermal gradient variation were computed, from where the geothermal gradient map (figure 4.7) was plotted. The results shows that geothermal gradients vary between 26.23°C/km and 73.60°C/km, most of the higher values are located at the North-Western. Highest values of 72°C/km and above are located at the mid of the of the north-western part of the study area, lowest values are found at the eastern part corresponding to the area of highest Curie point depth. This value of geothermal gradient agrees largely with Ofor and Udensi (2014) who recorded values that ranges between 26.18 to 44.62°C/km and Nwankwo and Shehu (2015) that obtained 20.84°C/km and 52.11°C/km

### 3.2.4 Heat Flow

Geothermal gradient which is the rate of increase in temperature per unit depth is a good indicator of

sub-surface temperature distribution and is significant in the assessment of geothermal energy resources of an area.-

The results (Table 4.1) shows that the heat flow (estimated in accordance with equation 8) values of the area varies between 65.84mW/m<sup>2</sup> and 184.74 mW/m<sup>2</sup>, from this results the heat flow contour (figure 4.6) was plotted.

Low values of 70 mW/m<sup>2</sup> to 110 mW/m<sup>2</sup> are located at the western region increasing to the central part and southwestern part, all this may be due to the presence of limestone, slate phyllite and pegmatite dominance (as indicated in Figure. 1) in this areas. While the higher value of 115 mW/m<sup>2</sup> to 180 mW/m<sup>2</sup> can be located at the extreme part of the North western part of the area of study, this high value might be as a result of igneous intrusion or the dominance of Alluvium and sandstone deposit in the area.

The result largely agreed with Ofor and Udensi (2014) that estimate the entire part of the study area.

The contour is closely related to the geothermal gradient map (Figure 4.8), meaning that most areas of high heat flow correspond to high geothermal gradient and vice versa.

The results have further reveal an almost inverse linear relationship between heat flow and Curie depths as predicted in equation 8.

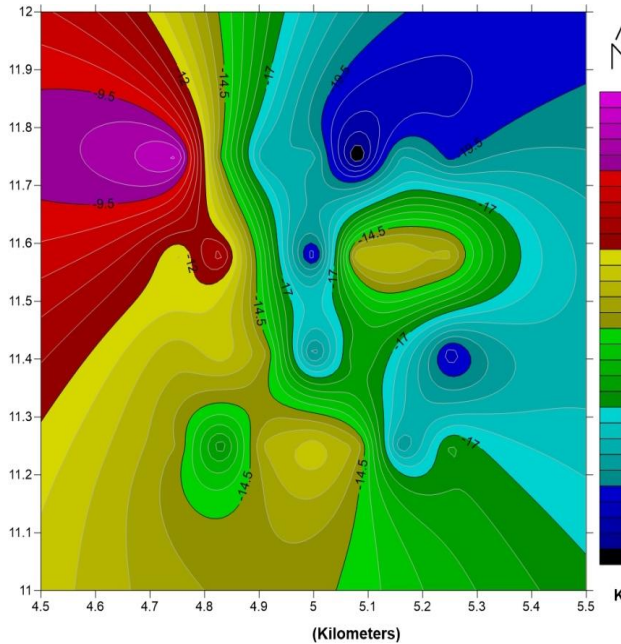


Figure. 4.4 contour map of the Curie point depth

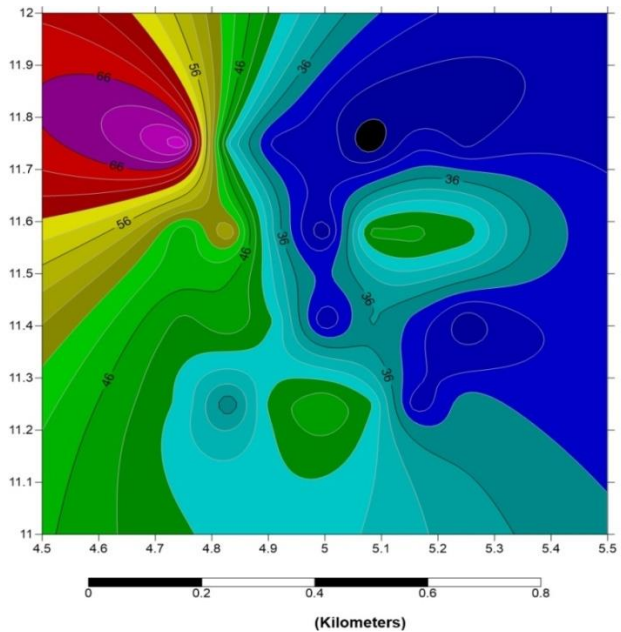


Figure. 4.5 contour map of the geothermal gradient

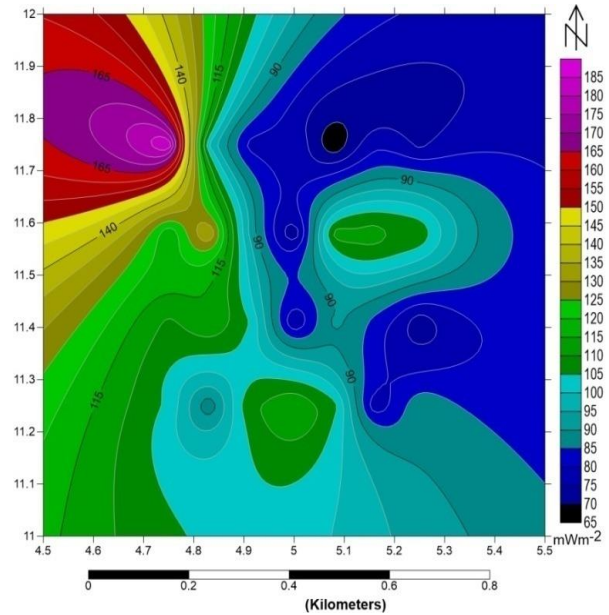


Figure. 4.6 contour map of the heat flow anomaly

#### 4.0 CONCLUSION

According to Jessop *et al.*, 1976; (Nwanko *et al* 2011) and Salako *et al* (2020), Generally, the units that comprise of high heat flow values always correspond to volcanic and metamorphic regions since the two rock units have high heat conductivities Jessop *et al.*, 1976; (Nwanko *et al* 2011) and Salako *et al* (2020)

The average heat flow in thermally normal continental region is reported to be above 60 mW/m<sup>2</sup>. However, values between 80 mW/m<sup>2</sup> and 100 mW/m<sup>2</sup> are considered to be good geothermal reservoir and values above 100 mW/m<sup>2</sup> is an indication of anomalous geothermal condition (Jessop *et al.*, 1976; Nwanko *et al* 2011; Ofor and Udensi, 2014; Nwankwo and Shehu (2015); Aliyu *et al* (2018) and Kamureyina (2019)).

This research have shown that the study area lies within the thermally normal continental regions and good geothermal source.

From the study it can be inferred that the geothermal prospect areas may be areas where thick blanket of thermally insulated sediments cover basement rocks since there is no evidence of volcanic activities in the study area, therefore these areas of high heat flow as shown in Figure 4.6 could be geothermal sources and reservoirs and will be of help in identifying the existence of productive

reservoirs at attractive temperature and depth in the Sokoto Basin.

### REFERENCES

- Aliyu, A. Salako, K. A. Adewumi, T. and Mohammed, A. (2018) Interpretation of High Resolution Aeromagnetic Data to Estimate the Curie Point Depth Isotherm of Part of Middle Benue Trough, North-East, Nigeria. *Physical Science International Journal* 17(3): 1-9
- Bhattacharyya, B.K. & Leu L.K. (1975). Spectral analysis of gravity and magnetic anomalies due to two-dimensional structures. *Geophysics* 40:993-1013
- Bhattacharyya, B.K., (1966). Continuous spectrum of the total magnetic field anomaly due to a rectangular prismatic body. *Geophysics*, 31, 97-121.
- Eletta, B.E., & Udensi, E.E. (2012). Investigation of Curie point isotherm from the magnetic field of Easter sector of central Nigeria. *Global journal of geosciences*. 101-106.
- Farhan H. (2013). Possibilities of Geothermal Energy and its Competitiveness with Other Energy Sources. Master's Thesis in Energy Engineering, faculty of engineering and sustainable development, University of Gavel.
- Fridleifsson I.B. and Dincer I. (2003) Status of geothermal energy amongst the world's energy sources. *Geothermics*; 32:379-88.
- Jessop, A. M, Habart, M. A and Sclater, J. G. (1976). The World heat flow data collection, 1975. *Geothermal services of Canada. Geothermal services*, 50, 55 -77.
- Kamureyina E., (2019) Geothermal Study Over Sokoto Basin Northwestern, Nigeria. *International Journal of Engineering Science Invention (IJESI)* 2319 – 6734
- Kasidi, S. and Nur, A. (2012). Curie depth isotherm deduced from spectral analysis of North-Eastern Nigeria. *Scholarly Journal of Biotechnology*. 49 -56.
- Kogbe, C.A (1979). Geology of the South Eastern (Sokoto) Sector of the Iullemeden Basin Bulletin, Department of Geology, Ahmadu Bello University, Zaria, Nigeria. 2 (1) 2.
- Kogbe, C.A. (1981). Cretaceous and Tertiary of the Iullemeden Basin in Nigeria (West Africa) *Cretaceous Research* 2, 129-186
- Megwara, J.U., Udensi, E.E., Olasehinde, P.I., Daniyan, M. A., & Lawal, K. M. (2013). Geothermal and radioactive heat studies of parts of southern Bida basin, Nigeria and the surrounding basement rocks. *International Journal of Basic and Applied Sciences*, 2 (1) 125-139
- Müjgan S., Oya P., Ilknur K. (2005) Determination of the Curie Point Depth and Heat Flow From Magsat Data of Western Anatolia. *Journal Of Balkan Geophysical Society*, Vol.8, No 4, p.149-160
- Nagata, T., (1961.) *Rock Magnetism*, 350 ., Maruzen, Tokyo,
- Nwankwo, L.I. and Shehu, Amada T. (2015) Evaluation of Curie-point depths, geothermal gradients and near-surface heat flow from high-resolution aeromagnetic (HRAM) data of the entire Sokoto Basin, Nigeria. *Journal of Volcanology and Geothermal Research*, Volume 305, p. 45-55.
- Nwankwo, L.I., P.I Olasehinde and C.O., Akaosile, 2011. Heat flow anomalies from the spectral analysis of airborne magnetic data of Nupe basin, Nigeria. *Asian Journal of earth sciences*. 1,3, 5-6.
- Obaje, N. G. (2009) Geology and mineral resources of Nigeria, *Lecture Notes in Earth Sciences*. Springer Berlin Heidelberg, 120, 77 -89.
- Odebo MO (2010). Sokoto Basin, Northwest Nigeria. *A Hand Book on Geology*.
- Ofor N.P. and Udensi E.E. (2014). Determination of the Heat Flow in the Sokoto Basin, Nigeria using Spectral Analysis of Aeromagnetic Data. *Journal of Natural Sciences Research* 4(6):83-93.
- Okubo, Y., Graf R. J., Hansen, R. O., Ogawa, K., & Tsu, H. (1985). Curie point depths of the Island of Kyushu and surrounding areas, Japan. *Geophysics*, 53(3), 481-494.
- Okubo, Y., Tsu, H., Ogawa, K. (1989). Estimation of Curie point temperature and geothermal structure of Island arc of Japan. *Tectonophysics*, 159, 279-290
- Ross H. E, Blakely R. J, Zoback M. D (2006) Testing the use of aeromagnetic data for the determination of Curie depth in California. *Geophysics*, 71(5), 51-59
- Salako, K. A., Adetona, A. A., Rafiu, A. A., Alahassan, U. D., Aliyu, A. and Adewumi, T. (2020) Assessment of Geothermal Potential of Parts of Middle Benue Trough, North-East

- Nigeria. *Journal of the Earth and Space Physics*, Vol. 45, No. 4, P. 27-42
- Spector, A., & Grant, F.S. (1970): Statistical models for interpreting aeromagnetic data. *Geophysics*, 35, 293 - 302.
- Stacey, F.D. (1977). *Physics of the Earth*. New York, NY, USA: John Wiley and Sons publication: 2nd edition.
- Tanaka, A., Okubo, Y., & Matsubayashi, O., (1999). Curie point depth based on spectral analysis of the magnetic anomaly data in East and South-East Asia. *Tectonophysics* 306, 461-470.
- Zboril L (1984). Sketch map of oil-bearing structures. *Geofyzika*, Brno, Czechoslovakia P 94.